Supplemental Information

Jeter et al., NANOG promotes cancer stem cell characteristics and prostate cancer resistance to castration

Supplemental Methods

Cells, reagents, and animals

Cancer cell lines including prostate (Du145, LNCaP and PC3 cells), breast (MCF-7) and colon (COLO320), teratocarcinoma cells (NTERA), and human embryonic kidney (HEK) 293T cells were obtained from ATCC (American Type Culture Collection, Manassas, VA, USA) and cultured in the recommended media. Xenograft human prostate tumors LAPC-4 and LAPC-9 were kindly provided by Dr. C. Sawyers (Klein *et al*., 1997; Reiter and Sawyers, 2001). NOD/SCID Interleukin-2 Receptor (IL2) knockout mice (NOD/SCID-γ) and NOD/SCID mice were obtained from the Jackson Laboratories (Bar Harbor, ME, USA) and maintained in standard conditions in the American Association for Accreditation of Laboratory Animal Care (AAALAC) approved MDACC Animal Facility. All chemicals were obtained from Sigma unless specified otherwise. Primary antibodies used in this study were summarized in Supplemental Table S2.

Purification of tumor cells from xenografts

Basic procedures have been described in our previous publications (Patrawala et al., 2006, 2007; Jeter et al., 2009; Li et al., 2009). In brief, xenograft prostate tumors (Du145, PC3, LAPC-4, and LAPC-9) were

harvested and minced into pieces and digested with 1x Accumax (Innovative Cell Technologies, Inc, San Diego, CA, USA). Dissociated cells were filtered through a 40-μm cell strainer (BD Falcon, Bedford, MA) and further separated from RBC and debris by Histopaque-1077 (Sigma-Aldrich, St. Louis, MO, USA) density gradient centrifugation. To deplete lineage-positive host cells, the crude tumor preparation was stained with biotinylated anti-$H2K^d$ (BD Pharmingen, San Jose, CA, USA) mouse haplotype marker and streptavidin-conjugated Qdot 655 (Invitrogen, Carlsbad, CA, USA). Separation was subsequently performed via FACS.

Tumor transplantation and castration

The basic procedures for subcutaneous (s.c) tumor cell implantation have been previously described (Patrawala et al., 2005, 2006, 2007). Briefly, NOD/SCID mice (6-8 week old) were injected s.c with different numbers of tumor cells in 50-μl of medium containing 50% Matrigel. Dorsal prostate (DP) orthotopic injections (25 μl) were performed as previously described (Patrawala et al., 2007; Li et al., 2009). Tumor development was monitored starting from the second week. Tumorigenicity was measured by tumor weight and tumor incidence. All animals were terminated at 1-5 months after tumor cell injection depending on tumor burden and morbidity. Tumors harvested were fixed in formalin and paraffin sections were cut for HE staining or IHC analysis. Castrations to assay androgen-independent growth *in vivo* were performed by surgical bilateral removal of the testis, vas deferens and testicular fat pad. Bicalutamide (5 mg/kg) intra-dermal injections were performed 3 days prior to the castration to further reduce androgen signaling.

Fluorescence-activated cell sorting (FACS) and ALDEFLUOR assays

GFP^+ and GFP^- ($7\text{-}AAD^-$ and Lin^-) tumor cells were sorted using a FACSAria flow cytometer (BD Biosciences, San Jose, CA, USA). ALDEFLUOR Assay (Stem Cell Technologies, Vancouver, Canada) was performed according to the manufacturers' protocol. In brief, trypsinized cells were suspended in

ALDEFLUOR Assay buffer and ALDEFLUOR substrate with or without the ALDH1 inhibitor diethylaminobenzaldehyde (DEAB). Following a 30-min. incubation at 37ºC, the stained cells were plunged into an ice bucket, centrifuged and re-suspended in ice-cold ALDEFLUOR Assay buffer, followed immediately by FACS analysis.

Immunofluorescence (IF) and immunohistochemistry (IHC) Staining

Basic procedures have been previously described (Jeter et al., 2009). IF detection of NANOG was performed via permeabilization and denaturation pretreatment (0.5% Triton X100, 0.25% sodium dodecyl sulfate). Fixed cells on coverslips were blocked with Background Sniper (Biocare Medical, Concord, CA, USA) for 15 min followed by the NANOG primary antibody (Santa Cruz Biotech, Santa Cruz, CA, USA) and incubated for 2 h at room temperature. Biotinylated anti-rabbit (Vector Laboratories, Burlingame, CA, USA) was used to amplify the signal followed by streptavidin-Alexafluor 594 (Invitrogen). CD133 staining was performed by incubating with a directly conjugated CD133-APC (Miltenyi Biotec). Coverslips were mounted in Prolong Gold Anti Fade (Invitrogen). Immunofluorescence images were captured either on an Olympus BX40 fluorescence microscope or a Zeiss confocal microscope.

For IHC, formalin fixed, paraffin-embedded tissue sections were deparaffinized and hydrated. Endogenous peroxidase activity was blocked (3% H_2O_2) and antigen retrieval was performed (10 mM citrate buffer; pH 6.0). After blocking with Biocare Blocking Reagent (Biocare), 1° antibodies (Supplemental Table S2) were incubated at appropriate dilutions for 30 min to 2 h at room temperature. Slides were washed in PBS twice and then incubated in biotinylated goat-anti-rabbit or mouse IgG (Vector Laboratories) at a 1:500 dilution for 30 min at room temperature, followed by streptavidin-conjugated horseradish peroxidase (BioGenex Laboratories Inc., San Ramon, CA) and DAB (BioGenex Laboratories Inc.) development.

In vitro proliferation, drug resistance, clonal, and clonogenic assays

pLVX cells, doxycycline-dosed as indicated, either alone or in the presence of the indicated drugs, were trypsinized and counted using a hemocytometer at the appropriate time point. BrdU staining procedures and basic clonal and clonogenic growth procedures have been previously described (Jeter *et al*., 2009; Li *et al*., 2009; Patrawala *et al*., 2006). To assay androgen-independent growth *in vitro*, androgen-deprivation was achieved by culturing cells in charcoal-dextran stripped serum (CDSS) and/or in 20 μM bicalutamide. For clonogenic assays, cells were plated at low density (ranging from 1-5K cells/well) in Methocult (StemCell Technologies) diluted according to manufacturers' specifications in DMEM/F12 plus B27 (Invitrogen) and N2 supplements (Invitrogen). Dissociated cells were added together with doxycycline (500 ng/ml) to the Methocult, mixed well and transferred to UltraLow Attachment 24-well dishes (Corning, Corning, NY, USA). Spheres (> 100 μm) that arose within 10-16 days were scored and imaged.

Migration assays

Migration properties of various pLVX LNCaP cells were observed via Biostation IM time-lapse video microscopy (Nikon, Melville, NY, USA). In brief, cells plated ~12 h prior and at 90% confluence were scored with a P20 pipette tip to generate a 'scratch'. Images were captured over the indicated time course. The NIS-Elements microscope imaging software system was used to analyze the videos and measure migration rates. A line with at least 3 cells intersecting was drawn across the field parallel to the scratch on each side to measure the initial distance apart (D1). At the appropriate time point (30 h later) a second set of parallel lines was drawn to measure the final distance apart (D2) and the distance traveled (μm) was calculated as D1-D2.

Supplemental References

Jeter CR, Badeaux M, Choy G, Chandra D, Patrawala L, Liu C *et al* (2009). Functional evidence that the self-renewal gene NANOG regulates human tumor development. *Stem Cells* **27:** 993-1005.

Klein KA, Reiter RE, Redula J, Moradi H, Zhu XL, Brothman AR *et al* (1997). Progression of metastatic human prostate cancer to androgen independence in immunodeficient SCID mice. *Nat Med* **3:** 402-8.

Li H, Jiang M, Honorio S, Patrawala L, Jeter CR, Calhoun-Davis T *et al* (2009). Methodologies in assaying prostate cancer stem cells. *Methods Mol Biol* **568:** 85-138.

Patrawala L, Calhoun T, Schneider-Broussard R, Li H, Bhatia B, Tang S *et al* (2006). Highly purified $CD44^+$ prostate cancer cells from xenograft human tumors are enriched in tumorigenic and metastatic progenitor cells. *Oncogene* **25:** 1696-708.

Patrawala L, Calhoun T, Schneider-Broussard R, Zhou J, Claypool K, Tang DG (2005). Side population is enriched in tumorigenic, stem-like cancer cells, whereas $ABCG2^+$ and $ABCG2^-$ cancer cells are similarly tumorigenic. *Cancer Res* **65:** 6207-19.

Patrawala L, Calhoun-Davis T, Schneider-Broussard R, Tang DG (2007). Hierarchical organization of prostate cancer cells in xenograft tumors: the $CD44^+\alpha2\beta1^+$ cell population is enriched in tumor-initiating cells. *Cancer Res* **67:** 6796-805.

Reiter RE, Sawyers CL (2001). Xenograft models and the molecular biology of human prostate cancer. In: Chung LWK, Isaacs WB and Simons JW (eds). *Prostate cancer: Biology, Genetics, and the New Therapeutics*. Humana Press Inc.: Totowa, NJ. pp 163-174.

Supplemental Figure Legends

Supplemental Figure S1: Fluorescence images and clonal analysis of PGK-GFP transduced Du145 cells.

a) LNCaP, Du145 and MCF-7 cells (50K/well in a 6-well dish) were transduced with the PGK-GFP or NP8-GFP reporters at 20-μl virus/well. Images (x100) were taken about one week after infection. Note that the majority of PGK-GFP infected cancer cells were positive for GFP whereas only a small percentage of cells infected with NP8-GFP were GFP^{+}.

b) PGK-$GFP^{+/-}$ Du145 cells exhibit similar cloning efficiency (C.E.). Du145 cells were infected with the respective lentiviruses (7 d) and viable ($7AAD^{-}$) GFP^{+}/GFP^{-} cells were purified by FACS and plated (200 cells/well in a 6-well dish). Colonies were counted 14 d later.

Supplemental Figure S2: Biological characterization of NP8-$GFP^{+/-}$ PCa cells in vitro and in vivo

a) NP8-GFP^{+} LNCaP cells exhibit higher clonal capacity in androgen-deprived conditions compared to the NP8-GFP^{-} cells. LNCaP cells transduced (7-10 d prior) with the NP8-GFP lentivirus were purified by FACS and plated either in regular media (200 cells/well), or in media supplemented with charcoal-dextran stripped serum (CDSS) or 20 μM bicalutamide. Colonies were stained with Giemsa and imaged at d 14.

b) IHC characterization of NP8-GFP^{+} versus NP8-GFP^{-} Du145 cell-derived tumors. Note that the NP8-GFP^{+} cell derived Du145 tumors contain more $NANOG^{+}$ and Ki-67+ cells. IHC staining with mouse IgG and rabbit (Rb) IgG was used as staining control for Ki-67 and NANOG staining, respectively.

Supplemental Figure S3: MCF7 cells transduced with pLVX-NANOGP8 or pLVX-NANOG1 express NANOG protein in the nucleus.

IF staining using a Rb polyclonal anti-NANOG antibody (H-155; Santa Cruz) revealed nuclear NANOG (red) following Dox induction (1 μg/ml, 48 h) in MCF7-pLVX-NANOG1/P8 cells. Note that in the absence of Dox, only a small percentage of MCF7 cells expressed NANOG protein, mostly on nuclear membrane and/or perinuclear regions. Original magnifications, x200.

Supplemental Figure S4: Diagram of promoter regions of NANOG target genes analyzed by ChIP

Arrows indicate the nucleotide positions of PCR primers relative to the transcription start site (TSS) used to amplify the chromatin-bound DNA associated with immunoprecipitated NANOG and the lengths of PCR products in base pairs (bp). Chromosomal locations of the promoters assayed and the gene name of the putative target are also indicated.

Supplemental Figure S5: Short-term NANOG overexpression in cancer cells is insufficient to promote proliferation or alter expression of proliferative or CSC markers.

a) NANOG induction does not increase LNCaP or Du145 cell numbers in 72 h. 50K cells of each type were plated in a 12-well dish and doxycycline dosed (μg/ml) as indicated. Cells were trypsinized and counted 72 h later and cell number (x1,000) is indicated.

b) BrdU incorporation assays. Cells indicated were treated with doxycycline for 3 days followed by a 4-h BrdU pulse. Staining was performed with Bu20A anti-BrdU mouse mAb and goat anti-mouse IgG conjugated to Alexafluor 594.

c-d) Western blot analysis. Cells (as indicated) were either un-induced or induced with doxycycline (500 ng/ml) for 3 d. Whole cell lysates were run on SDS-PAGE gels and Western blotting performed with the indicated antibodies (see Supplemental Table S2). In both experiments, N-tera cells were used as controls.

Supplemental Figure S6: Cellular and molecular characterizations of NANOG-overexpressing prostate tumors and PCa cells

a) qRT-PCR analysis of *Nanog* mRNA levels in LNCaP tumors in intact male mice (left) or Du145 s.c or DP tumors (right) derived from the pLVX-control, pLVX-NANOG1 or pLVX-NANOGP8 cells. The *Nanog* mRNA levels in pLVX-control tumors were set at 1. Bars represent the mean ± S.D (*n* = 2).

b) NANOG IHC staining in LNCaP tumors harvested in intact male NOD/SCID mice. The IHC staining was performed using a goat polyclonal anti-NANOG antibody (R & D) and under non-denaturing and non-amplified conditions to detect the transgene-derived NANOG protein (detection of endogenous NANOG protein in cancer cells requires denaturation and amplifications; see Jeter *et al*., 2009).

c) Ki-67 staining in pLVX-control versus pLVX-NANOG1/P8 LNCaP cell-derived tumors in intact NOD/SCID-γ mice. Original magnifications, x200.

d) NANOG1/P8 overexpression in Du145 cells increases ALDEFLUOR-positive cells. The three types of Du145 cells as indicated were treated with doxycycline (500 ng/ml) for 10 d and then used in Aldefluor assays.

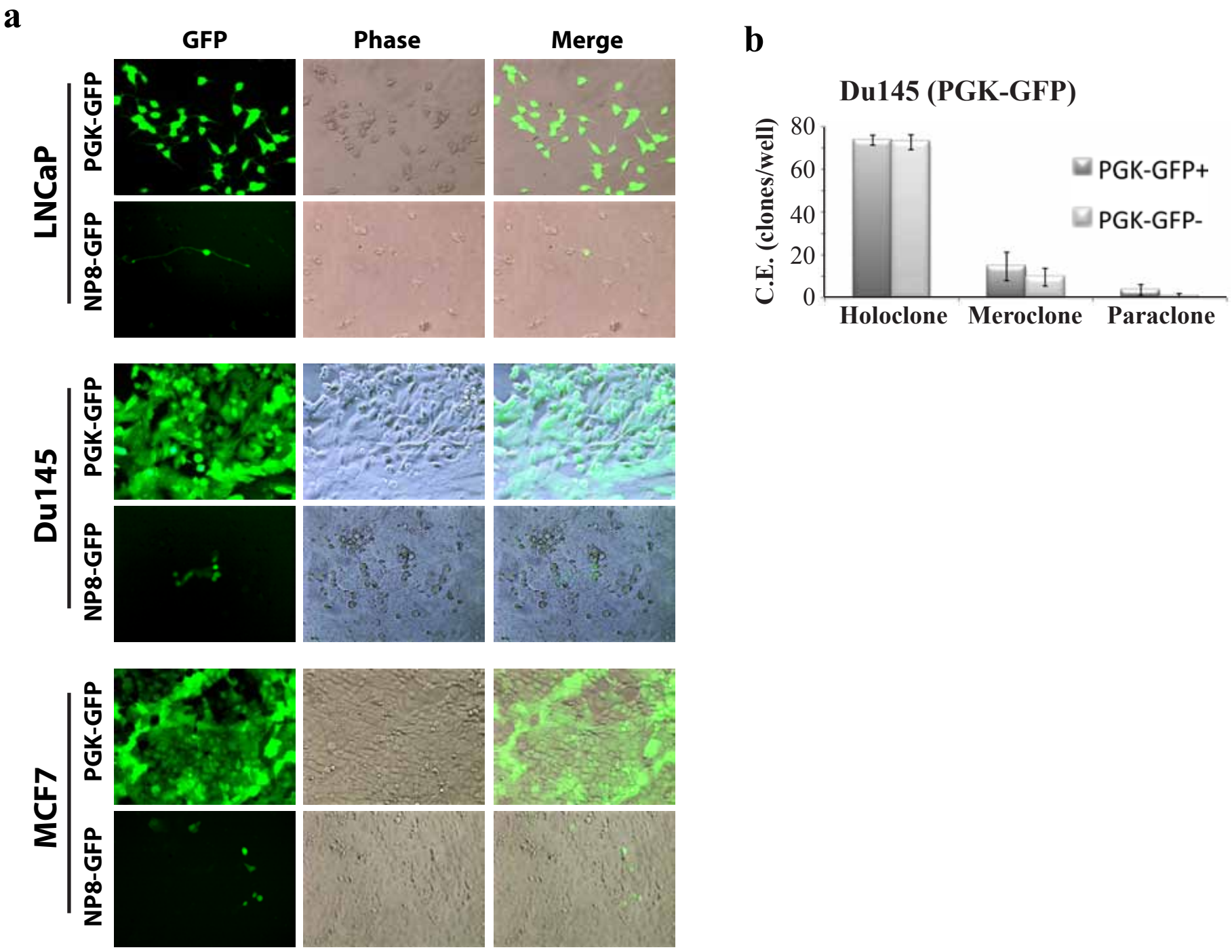
a
GFP
Phase
Merge
LNCaP
PGK-GFP
NP8-GFP
Du145
PGK-GFP
NP8-GFP
MCF7
PGK-GFP
NP8-GFP
b
Du145 (PGK-GFP)
C.E. (clones/well)
80
60
40
20
0
PGK-GFP+
PGK-GFP-
Holoclone
Meroclone
Paraclone

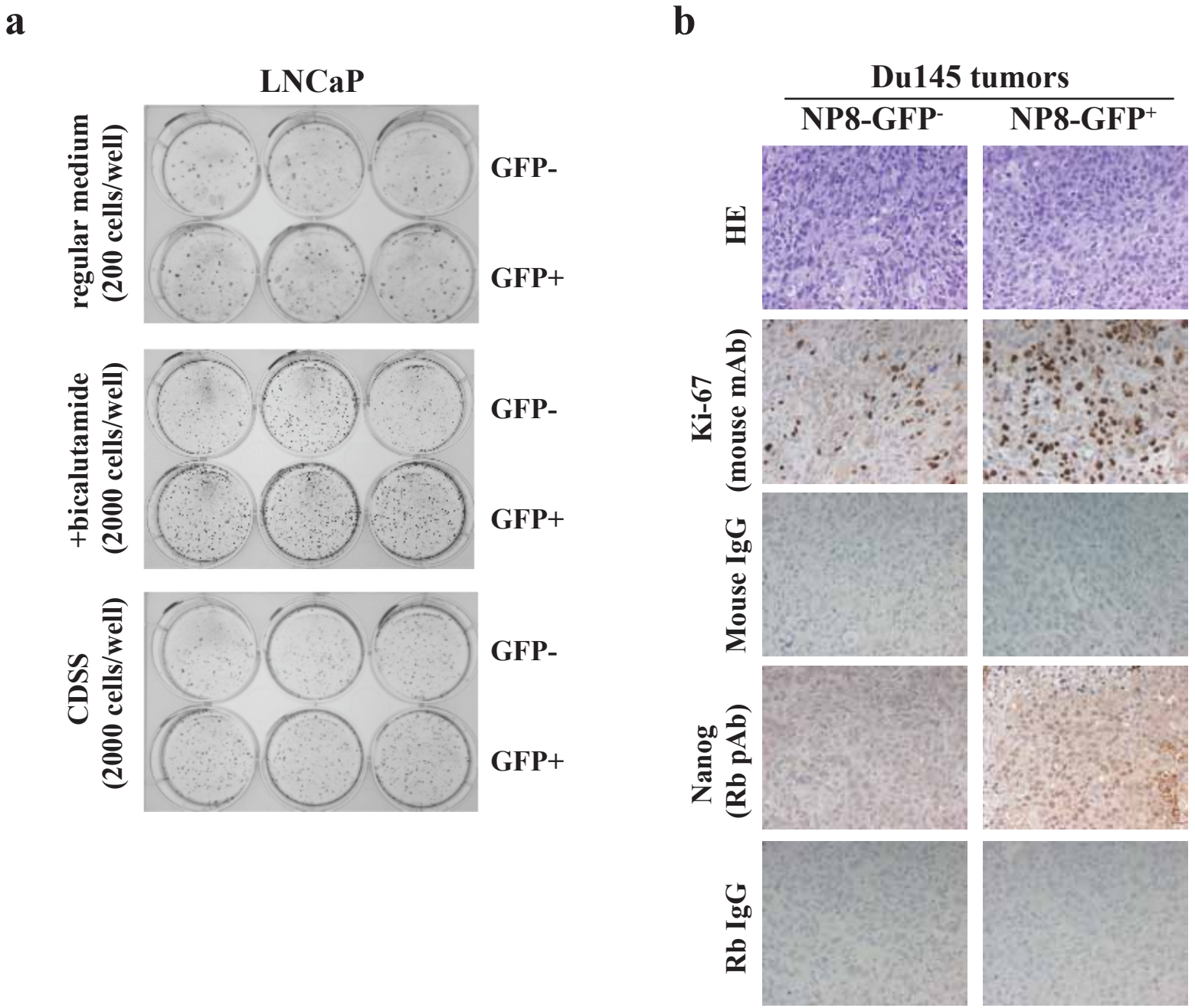
a
LNCaP
regular medium (200 cells/well)
GFP-
GFP+
+bicalutamide (2000 cells/well)
GFP-
GFP+
CDSS (2000 cells/well)
GFP-
GFP+
b
Du145 tumors
NP8-GFP-
NP8-GFP+
HE
Ki-67 (mouse mAb)
Mouse IgG
Nanog (Rb pAb)
Rb IgG

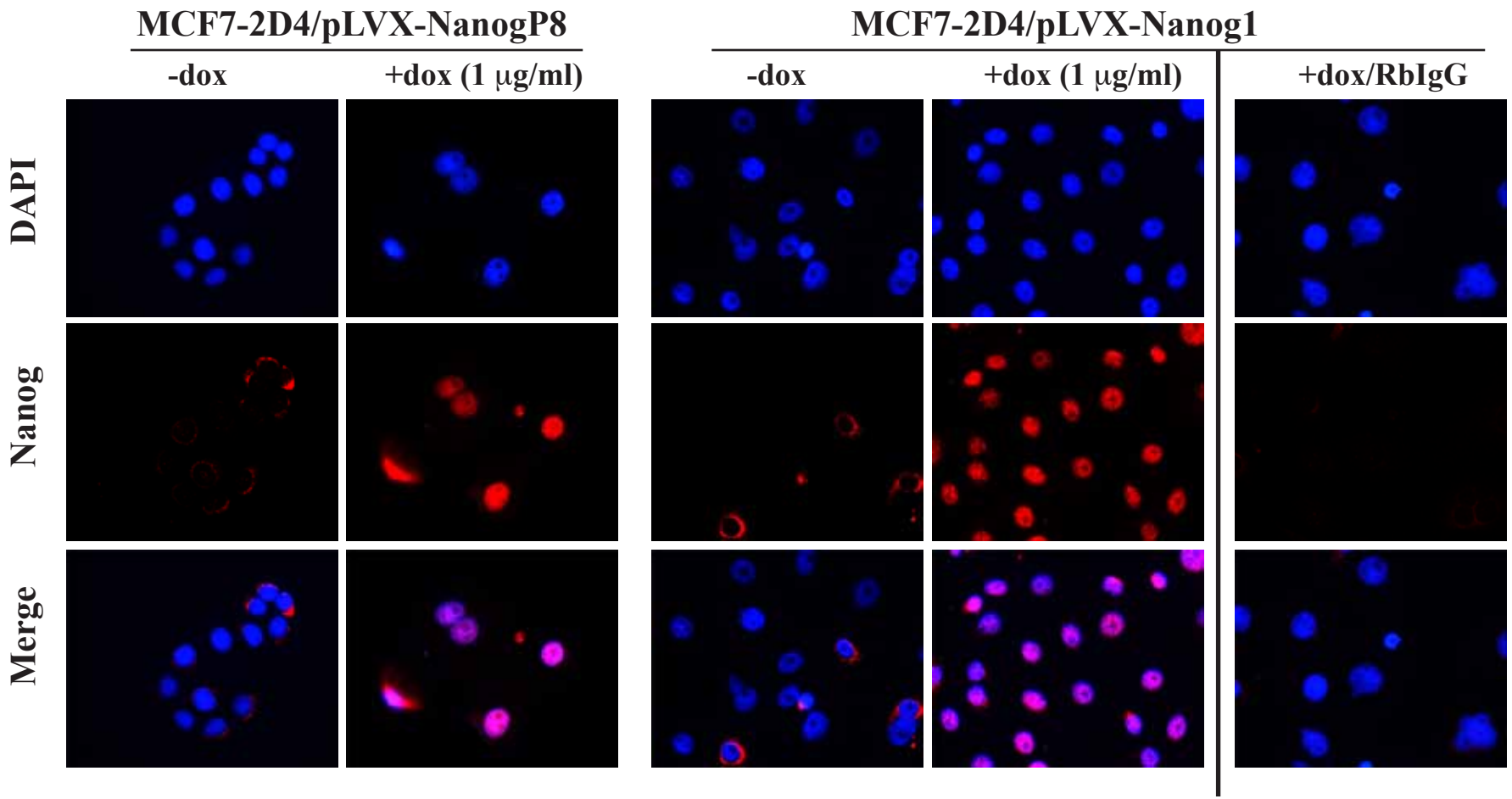
MCF7-2D4/pLVX-NanogP8
MCF7-2D4/pLVX-Nanog1
-dox
+dox (1 μg/ml)
-dox
+dox (1 μg/ml)
+dox/RbIgG
DAPI
Nanog
Merge

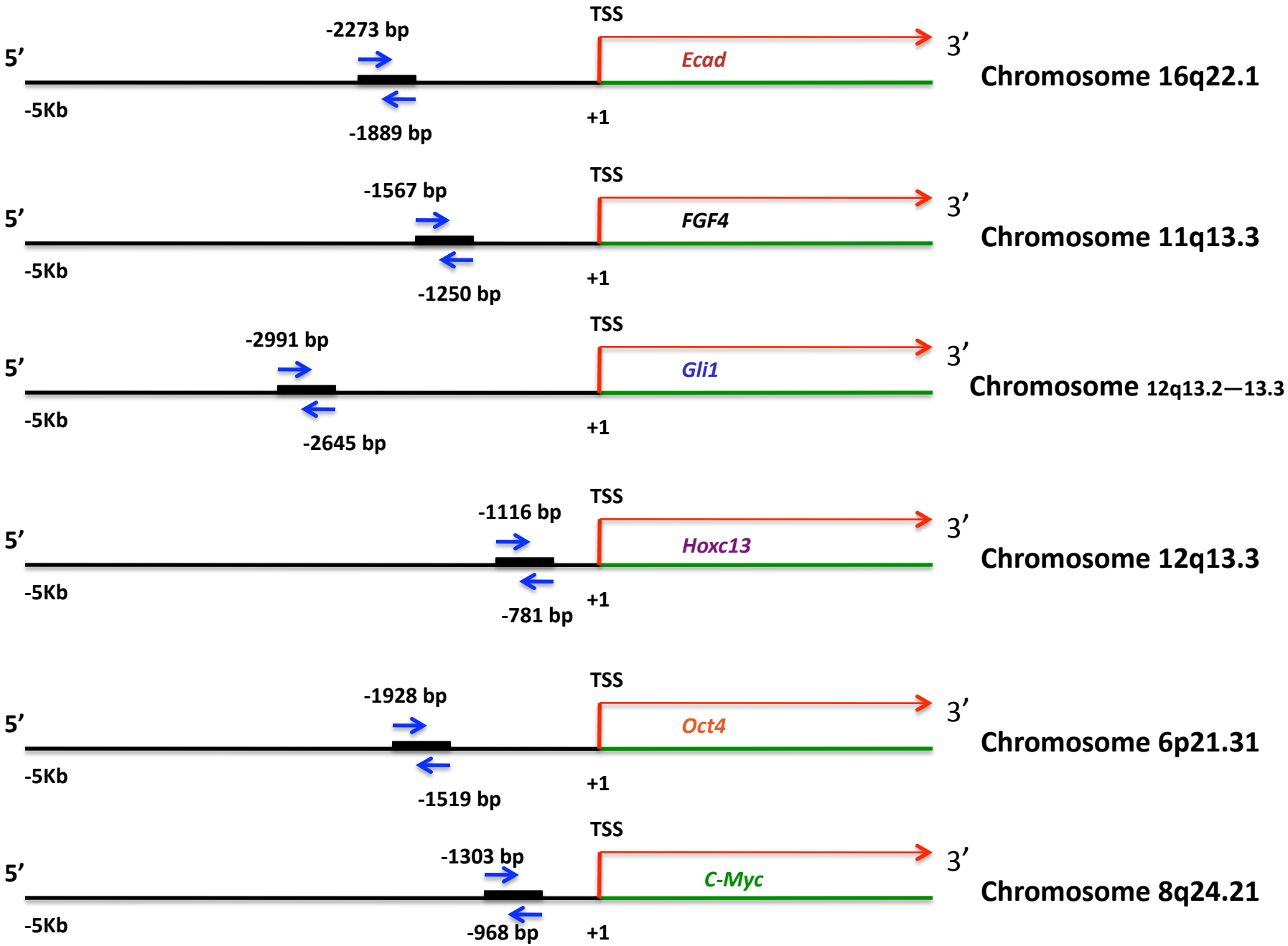
TSS
-2273 bp
5'
Ecad
3'
Chromosome 16q22.1
-5Kb
+1
-1889 bp
TSS
-1567 bp
5'
FGF4
3'
Chromosome 11q13.3
-5Kb
+1
-1250 bp
TSS
-2991 bp
5'
Gli1
3'
Chromosome 12q13.2—13.3
-5Kb
+1
-2645 bp
TSS
-1116 bp
5'
Hoxc13
3'
Chromosome 12q13.3
-5Kb
+1
-781 bp
TSS
-1928 bp
5'
Oct4
3'
Chromosome 6p21.31
-5Kb
+1
-1519 bp
TSS
-1303 bp
5'
C-Myc
3'
Chromosome 8q24.21
-5Kb
+1
-968 bp

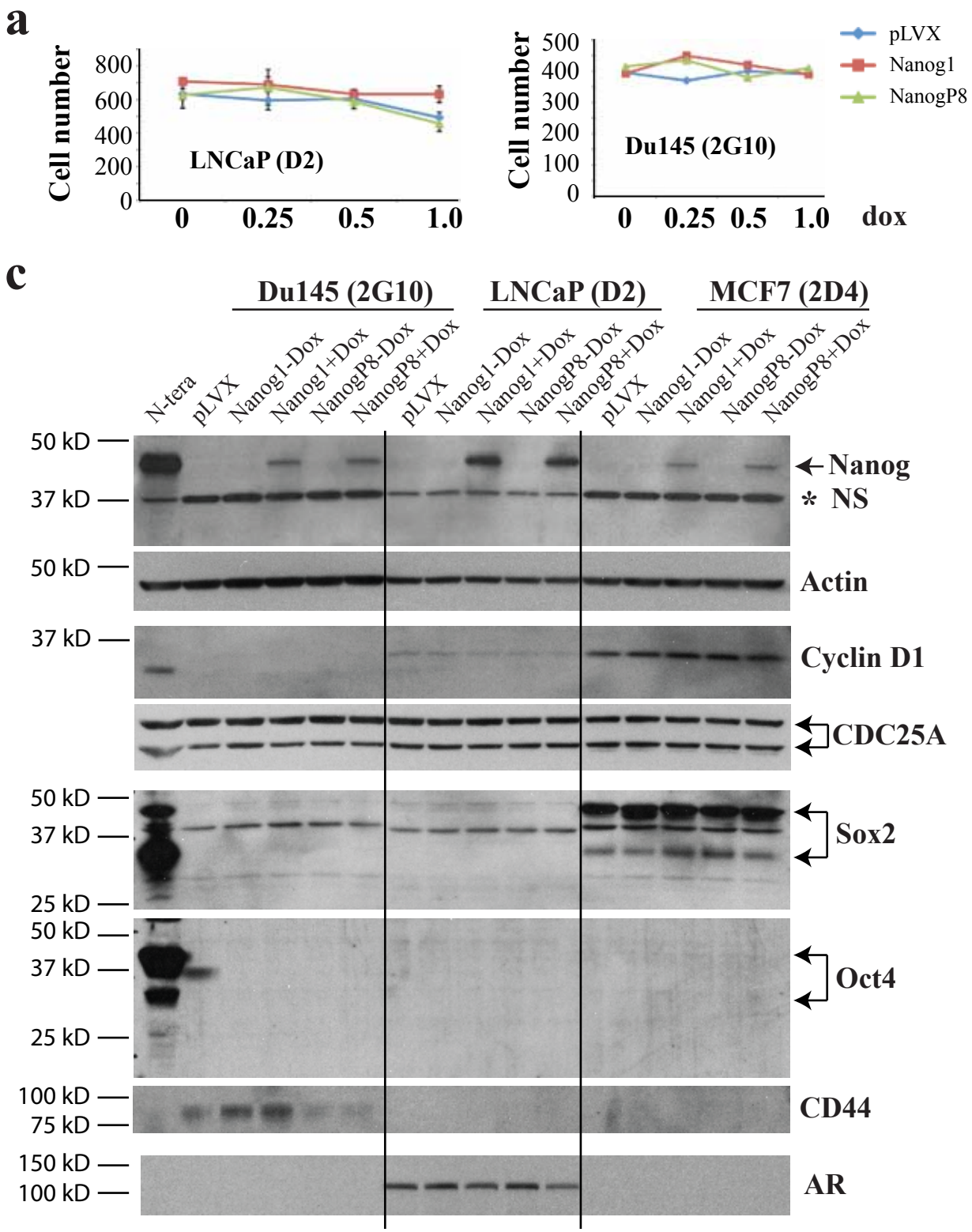
a
Cell number
LNCaP (D2)
Du145 (2G10)
dox
pLVX
Nanog1
NanogP8
b
LNCaP
Du145
% BrdU+ cells
pLVX
Nanog1
NanogP8
c
Du145 (2G10)
LNCaP (D2)
MCF7 (2D4)
N-tera
pLVX
Nanog1-Dox
Nanog1+Dox
NanogP8-Dox
NanogP8+Dox
Nanog
* NS
Actin
Cyclin D1
CDC25A
Sox2
Oct4
CD44
AR
d
LNCaP (D2)
pLVX-Dox
pLVX+Dox
CDK6
c-Myc
Gli-1
Snail
E-cadrin
*NS
Nkx3.1

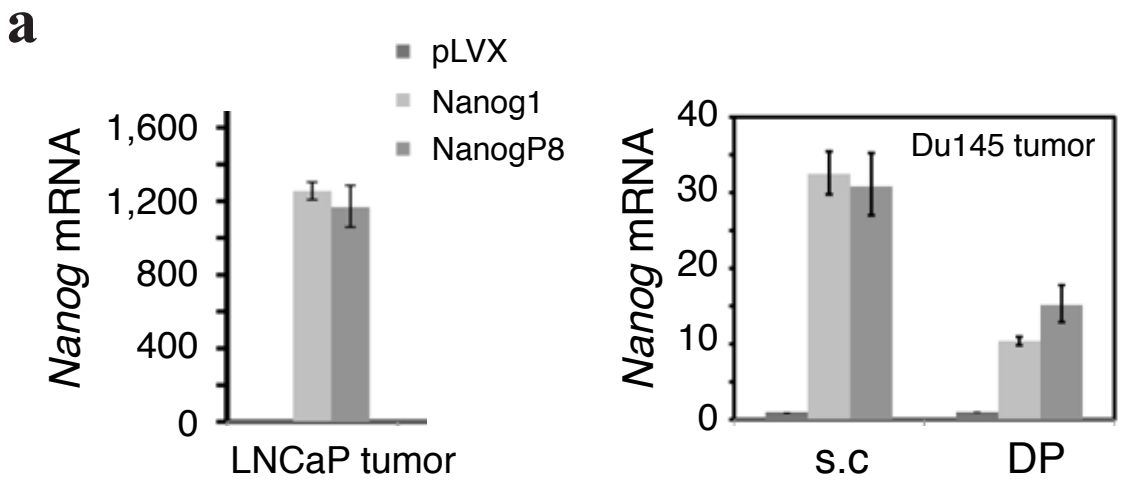
a
pLVX
Nanog1
NanogP8
Nanog mRNA
1,600
1,200
800
400
0
LNCaP tumor
Nanog mRNA
40
30
20
10
0
Du145 tumor
s.c
DP

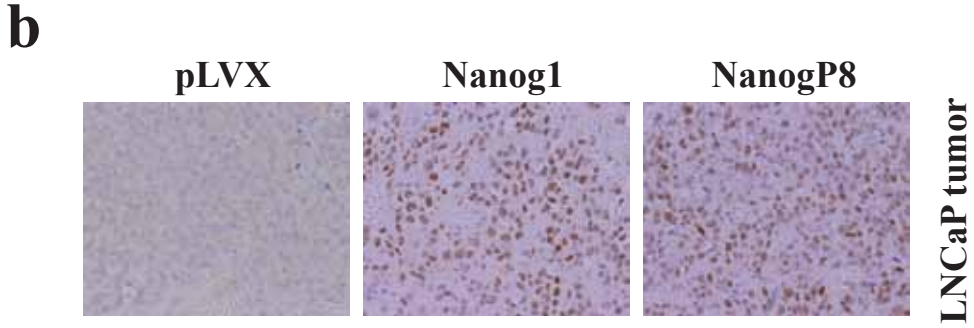
b
pLVX
Nanog1
NanogP8
LNCaP tumor

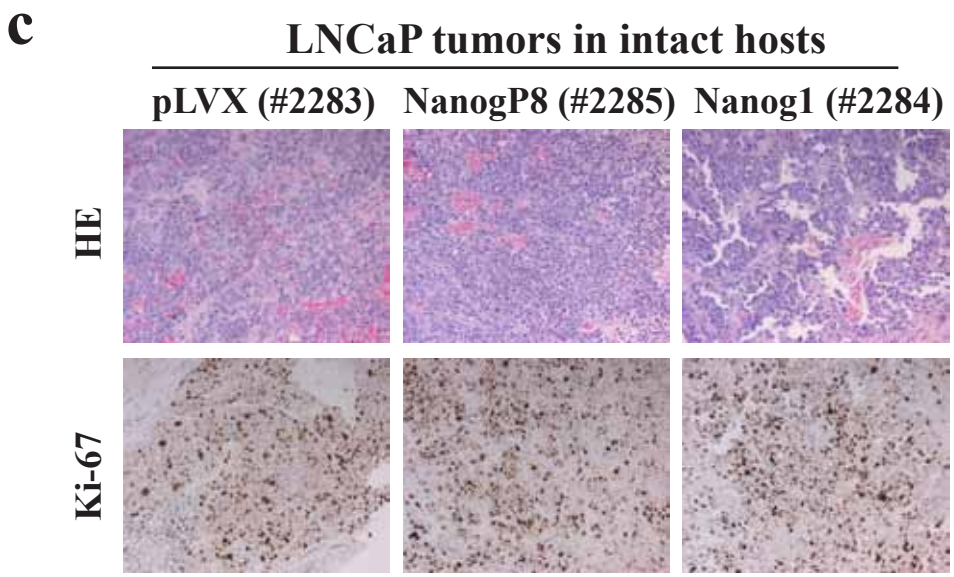
c
LNCaP tumors in intact hosts
pLVX (#2283)
NanogP8 (#2285)
Nanog1 (#2284)
HE
Ki-67

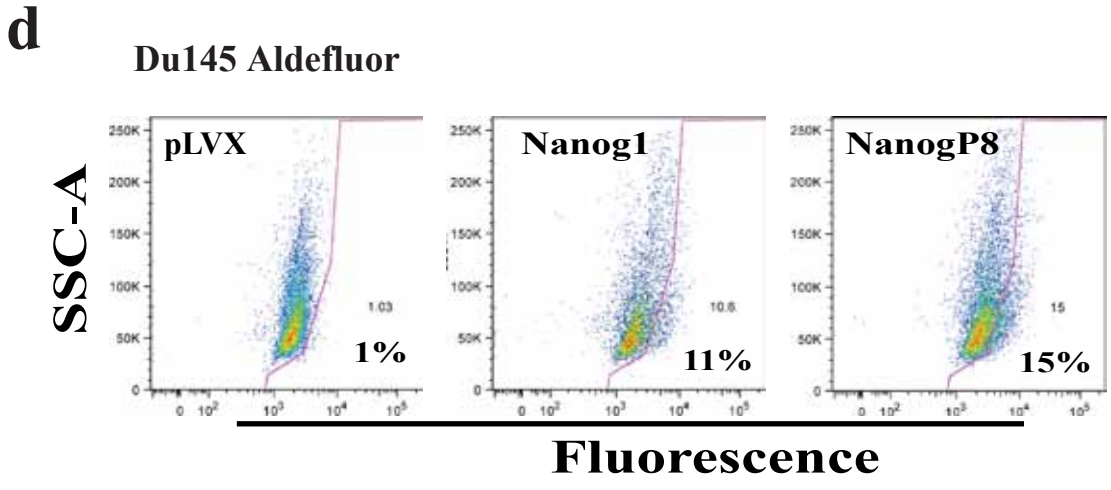
d
Du145 Aldefluor
SSC-A
pLVX
1%
Nanog1
11%
NanogP8
15%
Fluorescence

Supplemental Table S1. qPCR (TaqMan or SYBR Green) primer/probe sequences

TaqMan
Primer/probe sequences

mRNA		F primer	R primer	Probe
GAPDH		Cat# 4352339E		
Nanog1		CGCCCTGCCTAGAAAAGACATTT	AGAAGCCGTCTCTGGCTATAGATAA	CTGCTAAGGACAACATTGAT*
NanogP8		CGCCCTGCCTAGAAAAGACATTT	ACGAGTTTGGATATCTTTAGGGTTTAGAATC	CCTTGGCTGCCGTCTCTG*

For Nanog1-specific qPCR, the probe spans a portion of the 23-bp region in the 3'UTR unique to Nanog1mRNA (see Figure 1A).
For NanogP8-specific qPCR, the probe spans the upstream and downstream regions flanking the 23-bp region (junction site).
*FAM-MGB

SYBR Green
Primer sequences

mRNA	Accession	Forward Primers	Reverse Primers
α2-integrin	NM_002203.3	CCGACAAATACCAGCTGCTCAAG	TCCAGTGTTGTATGCACTTTCCC
ABCG2	NM_004827.2	ACAACCATTGCATCTTGGCTGTC	GCTGCAAAGCCGTAAATCCATATC
ALDH1A1	NM_000681.3	ACAGAGACAATTTAAGGCCTGCAC	ACAGACAAGAGGACCACTCCATTC
β1INTG	NM_002211.3	TGTGGGTGGTGCACAAATTCAAC	TCATCACATCGTGCAGAAGTAGGC
BCL2	NM_000633.2	CTGGGATGCCTTTGTGGAACTG	AGTCTTCAGAGACAGCCAGGAG
CD44	NM_000610.3	AGACAACCACAAGGATGACTGATG	TCCAGTTTCCTTCATAAGCAGTGG
cKIT (CD117)	NM_000222.2	TGTCGCTGTAAAGATGCTCAAGCC	AGTTCAGACATGAGGGCTTCCC
C-MYC	NM_002467	TTCTCTCCGTCCTCGGATTCTCTG	TCTTCTTGTTCCTCCTCAGAGTCG
CXCR4	M_001008540	TCCTGGCTTTCTTCGCCTGTTG	TGAAGGAGTCGATGCTGATCCC
CDH1 (E-cad)	NM_004360.3	AGAACGCATTGCCACATACACTC	ACTGCATTCCCGTTGGATGACAC
IGFBP5	NM_000599.3	TACCGCGAGCAAGTCAAGATCGAG	CTTCACTGCTTCAGCCTTCAGCTC
MMP9	NM_004994.2	ACGTGAACATCTTCGACGCCATC	TCAGAGAATCGCCAGTACTTCCC
NANOG	NM_024865.2	TAGCAATGGTGTGACGCAGAAG	TCTGGTTGCTCCACATTGGAAGG
OCT-4	NM_002701.4	GAGGCAACCTGGAGAATTTGTTCC	ATGTGGCTGATCTGCTGCAGTG
CD133 (PROM1)	NM_006017.2	ACAATTCACCAGCAACGAGTCC	GACGCTTTGGTATAGAGTGCTCAG
SNAIL1	NM_005985.2	CCAATCGGAAGCCTAACTACAGC	GCTGCTGGAAGGTAAACTCTGG
SOX2	NM_003106.2	CATCACCCACAGCAAATGACAGC	TTGCGTGAGTGTGGATGGGATTG
TWIST1	NM_000474.3	ACAAGCTGAGCAAGATTCAGACC	TTGCCATCTTGGAGTCCAGCTC

Supplemental Table S2: Primary antibodies used in the present study

Antibody Specificity	Company	Catalogue #	Host/Type	Application
Nanog	Kamiya Biomedical Company	PC-102	rabbit polyclonal	WB
Nanog	Santa Cruz Biotechnology	sc-33759	rabbit polyclonal	WB/IF/IHC
C-Myc	Santa Cruz Biotechnology	sc-40	mouse monoclonal	WB
Gli-1	Santa Cruz Biotechnology	sc-20687	rabbit polyclonal	WB
AR	Santa Cruz Biotechnology	sc-7305	mouse monoclonal	WB/IHC
IGFBP-5	Santa Cruz Biotechnology	sc-6006	goat polyclonal	WB
E-Cadherin	Santa Cruz Biotechnology	sc-7870	rabbit polyclonal	WB
PSA	Santa Cruz Biotechnology	sc-7316	mouse monoclonal	WB/IHC
Snail	Cell Signaling Technology	#3895	mouse monoclonal	WB
Slug	Cell Signaling Technology	#9585	rabbit monoclonal	WB
Phospho-ERK1/2	Cell Signaling Technology	#9101	rabbit polyclonal	WB
Phospho-STAT3	Cell Signaling Technology	#9145	rabbit polyclonal	WB
ERK1	Santa Cruz Biotechnology	sc-93	rabbit polyclonal	WB
ERK2	Santa Cruz Biotechnology	sc-1647	mouse monoclonal	WB
STAT3	Cell Signaling Technology	#9132	rabbit polyclonal	WB
OCT-4	Chemicon International	MAB4306	mouse monoclonal	WB
SOX-2	Chemicon International	AB5603	rabbit polyclonal	WB
CDK6	Santa Cruz Biotechnology	sc-177	rabbit polyclonal	WB
NKX3.1	Abcam	ab78008	rabbit polyclonal	WB
Cdc25A	Santa Cruz Biotechnology	sc-97	rabbit polyclonal	WB
CyclinD1	Santa Cruz Biotechnology	sc-717	rabbit polyclonal	WB
β-actin	Sigma	A-5441	mouse monoclonal	WB
CD44	Abcam	ab51037	mouse monoclonal	WB
CD133 (APC)	Miltenyi Biotec	130-090-826	mouse monoclonal	IF
Ki-67	Dako	M-7249	rat polyclonal	IHC

Supplemental Table S3: qRT-PCR
Quantification of relative mRNA levels in response to NANOG overexpression

Shown are the mean mRNA values in pLVX-Nanog1 (N1) or pLVX-NanogP8 (NP8) relative to pLVX control
Red: upregulation >2X (200%); Blue: downregulation < 0.5X (50%)
Underlined indicates fold change > 2x (or less than 0.5X) with P <0.05

LNCaP spheres, AI conditions (CDSS) and + bicalutamide (bic)

Gene	LNCaP N1 Spheres	LNCaP NP8 Spheres	LNCaP N1 AI	LNCaP NP8 AI	LNCaP N1 Bic	LNCaP NP8 Bic
IGFbp5	0.9100	0.8186	**2.7712**	**3.4917**	**5.3649**	**6.9555**
CXCR4	**0.4820**	**0.4525**	**2.9874**	**2.2719**	**11.5014**	**9.6778**
CD133	**5.6978**	**4.9888**	1.2616	1.0097	1.1792	1.4547
ABCG2	**3.1930**	**2.9834**	1.3857	1.0247	1.6881	1.9427
cKIT	**4.1073**	**2.4193**	1.5513	0.5305	0.8123	1.1454
TWIST	1.8778	1.0831	0.9848	0.7418	1.6121	1.3219
SOX2	0.5401	0.5294	1.1952	1.0390	0.6420	0.8253
SNAIL	1.0095	0.8613	0.9997	1.2009	0.8371	0.9815
a2INTG	0.8926	0.9239	1.4272	1.2698	0.6310	0.8630
eCAD	1.2990	1.2040	0.9186	0.8662	0.5652	0.5403
OCTA4	0.8121	0.9045	1.1952	1.0390	0.6420	0.8253

LNCaP 72h, 7d and 14d, standard culture conditions

Gene	LNCaP N1 72h	LNCaP NP8 72h	LNCaP N1 7d	LNCaP NP8 7d	LNCaP N1 14d	LNCaP NP8 14d
IGFbp5	1.8900	**2.2500**	**3.5751**	**3.9866**	**4.1834**	**3.3764**
CXCR4	1.7670	**5.9920**	**2.1765**	**2.6681**	1.4397	0.7113
CD133	**2.6760**	**2.7260**	**2.3072**	1.6234	1.4174	1.4912
ABCG2	1.1603	1.3966	1.9175	1.5901	**2.3979**	**2.1487**
cKIT	**2.8050**	1.5290	1.9828	1.2315	1.1197	0.8295
TWIST	0.9152	**5.5840**	1.2993	0.8689	1.6469	1.6869
SOX2	0.8750	**2.6900**	1.7854	1.0589	1.3391	1.1578
SNAIL	1.0270	1.0120	1.4483	1.1010	1.1517	1.1462
a2INTG	0.8761	0.9818	1.3688	1.0457	1.3214	1.2266
eCAD	1.0286	1.0515	1.2359	0.8815	1.0596	0.9837
OCTA4	0.8593	1.0960	1.1738	1.0739	1.0244	0.8205

MCF7 72h, 5d and 14d, standard culture conditions

Gene	MCF7 N1 72h	MCF7 NP8 72h	MCF7 N1 5d	MCF7 NP8 5d	MCF7 N1 14d	MCF7 NP8 14d
ALDH1A1	1.2409	0.6121	**3.8762**	**2.8082**	1.4950	**4.5079**
MMP9	1.1842	1.2657	**2.2267**	1.1864	**2.7468**	**3.0160**
CD133	**2.4281**	1.5013	0.9907	1.2304	**2.2773**	**2.4706**
cMYC	**2.0999**	**2.0243**	1.1345	0.8447	**2.0327**	**2.0158**
ABCG2	0.7743	0.6056	1.4176	1.0405	**2.2876**	1.9762
CD44	**3.3247**	1.9783	1.0844	0.7895	1.9733	**2.3349**
TWIST	**2.1662**	**2.3250**	**2.2362**	**2.0539**	1.6965	1.1801
cKIT	**0.4302**	**0.4718**	1.6855	1.1173	0.9240	**2.8926**
BCL2	0.7197	0.7360	1.3943	1.2490	1.5370	1.6252
OCTA4	1.1835	1.0563	1.1465	0.9528	1.7328	1.8650
b1INTG	1.0701	0.6346	1.3064	0.9719	1.8270	1.6572
SOX2	0.7802	0.6200	1.1944	1.0254	1.5174	1.7138
SNAIL	1.4500	1.5178	1.5473	1.2574	1.5501	1.6842
a2INTG	1.3808	1.1861	0.9523	0.8390	1.2932	1.4472

Du145 7d, standard culture conditions

Gene	DU145 N1 7d	DU145 NP8 7d
TWIST	**6.7377**	**11.0187**
ALDH1	1.7287	**2.6154**
CD133	**2.0506**	**2.2199**
BCL2	1.3931	1.7695
CXCR4	1.4474	1.5499
a2INTG	1.1054	1.2346
eCAD	1.3261	1.2591
IGFbp5	0.8385	0.8401
OCTA4	0.6945	1.0696
SOX2	1.0895	1.2348
SNAIL	0.9779	1.0592